Available online at www.sciencedirect.com
ScienceDirect
Planetary and Space Science 54 (2006) 1457–1471
Planetary and Space Science
www.elsevier.com/locate/pss

Venus O^+ pickup ions: Collected PVO results and expectations for Venus Express

J.G. Luhmann[a,*], S.A. Ledvina[a], J.G. Lyon[b], C.T. Russell[c]

[a]SSL, 7 Gauss Way, University of California, Berkeley, CA 94720-7450, USA
[b]Department of Physics and Astronomy, Dartmouth College, Hanover, NH 03755, USA
[c]IGPP/UCLA, Los Angeles, CA 90095-1567, USA

Received 3 December 2004; received in revised form 25 October 2005; accepted 28 October 2005
Available online 19 January 2006

Abstract

Observations of oxygen pickup ions by the plasma analyzer on the Pioneer Venus Orbiter (PVO) Mission arguably launched broad interest in solar wind erosion of unmagnetized planet atmospheres, and its potential evolutionary effects. Oxygen pickup ions may play key roles in the removal of the oxygen excess left behind from the photodissociation of water vapor by enabling direct escape, additional sputtering of oxygen when they impact the exobase, and escape as energetic neutrals produced in charge exchange reactions with the ambient exospheric oxygen and hydrogen. Although the PVO observations were compromised by an ~8 keV energy limit for O^+ detection, a lack of ion composition capability, and the limited sampling and data rate of the plasma analyzer which was designed for solar wind monitoring, these measurements provide our best information about the extended O^+ exosphere and wake at Venus. Here we show the full picture of the spatial distribution and energies of the O^+ ion observations collected by the plasma analyzer during PVO's ~5000 orbit tour. A model of O^+ test particles launched in the circum-Venus fields described by an MHD simulation of the solar wind interaction is used to help interpret the PVO observations and to anticipate the expanded view of Venus O^+ escape that will be provided by the ASPERA-4 experiment on Venus Express.

Keywords: Venus; Atmosphere escape; Pickup ions; Venus express

1. Introduction

While the loss of the atmosphere of the planet Mars, past and present, has become the current subject of intense interest, many of the concepts being applied to Mars had their origins in earlier studies of the Venus upper atmosphere inspired by Pioneer Venus Orbiter (PVO) observations (e.g. see Luhmann and Bauer, 1992 and references therein). Venus retains a substantial atmosphere, but Venus, like Mars, is water-poor compared to Earth. Of the constituents of water, light hydrogen escapes relatively easily from the planet's gravitational well. Indeed, photodissociation of copious quantities of H_2O in the upper atmosphere, supplied by the vaporization of all surface ice or water, must have produced an extreme early escape scenario for hydrogen during the first few hundred million years of the planet's life. This hydrodynamic escape (e.g. Chamberlain and Hunten, 1987) may moreover have dragged with it heavier constituents, including the oxygen produced by the photodissociation of water, but the potential problem of excess oxygen build-up over time after this phase has never been satisfactorily resolved. Residual oxygen can either be taken up by the crust or escape to space. Mass 16 atoms or ions require at least ~10 eV of energy to escape from Venus, more than is typically available from the photochemical processes in the ionosphere. Though exothermic dissociative recombination of ionospheric O_2^+ produces the hot oxygen corona, few particles with the required >11 km/s velocities result (e.g. Nagy et al., 1981). Yet observations suggest that the current amount of surface oxidation cannot account for the left over oxygen. Thus, the Pioneer Venus Orbiter plasma analyzer observational evidence for O^+ escape into the

*Corresponding author. Tel.: +1 510 642 2545; fax: +1 510 643 8302.
E-mail address: jgluhman@ssl.berkeley.edu (J.G. Luhmann).

0032-0633/$ - see front matter © 2005 Elsevier Ltd. All rights reserved.
doi:10.1016/j.pss.2005.10.009

solar wind (Mihalov and Barnes, 1981; Intriligator, 1989), also inferred from earlier Venera spacecraft measurements (Vaisberg et al., 1976), raised further interest in the escape process.

The solar wind interaction provides a mechanism by which oxygen ions can easily attain the >11 km/s outward velocities required for escape. Its magnetic field and motional electric field penetrate the upper atmosphere and oxygen corona above the ionopause, accelerating any ions created there by photoionization, impact by solar wind electrons, or charge exchange with solar wind ions. The resulting O^+ ion trajectories carry them anti-Sunward.

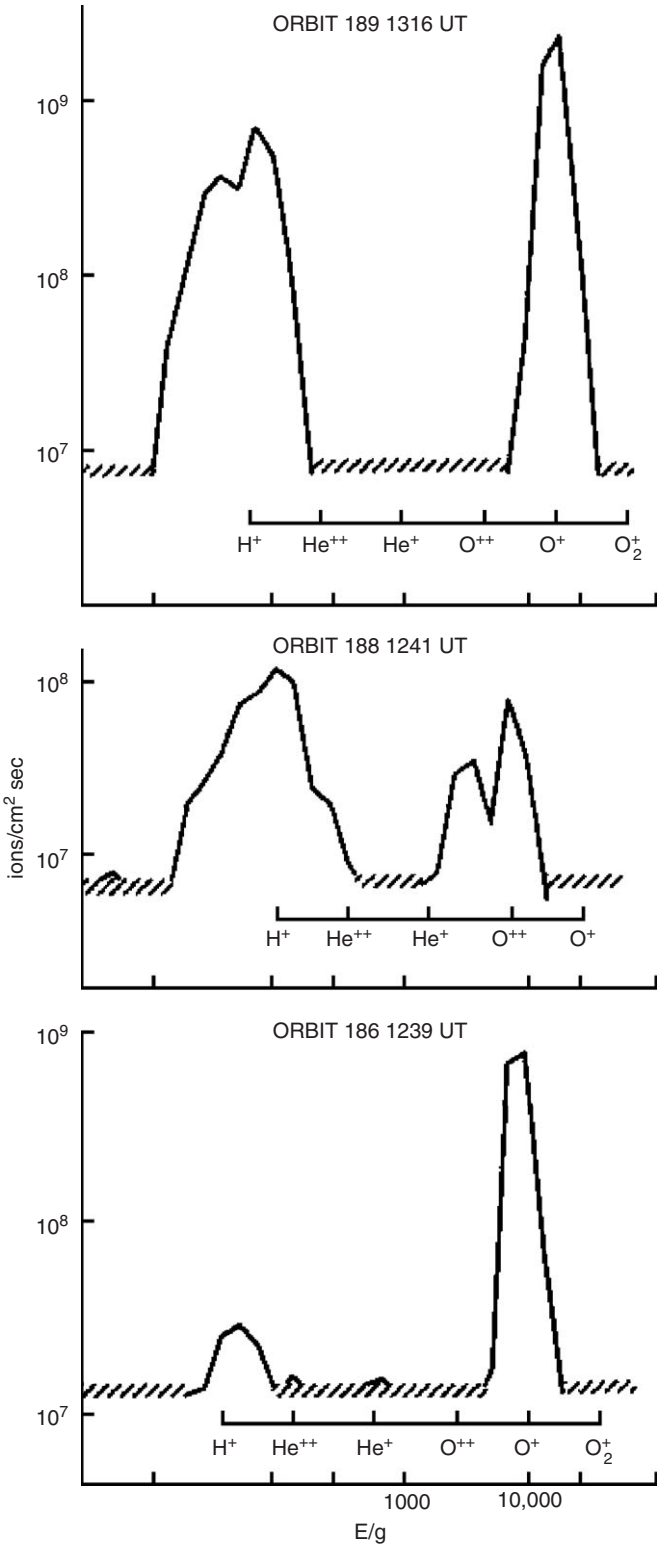

Fig. 1. Sample E/q spectra from the PVO Plasma Analyzer (OPA). Reproduced from Mihalov and Barnes (1981).

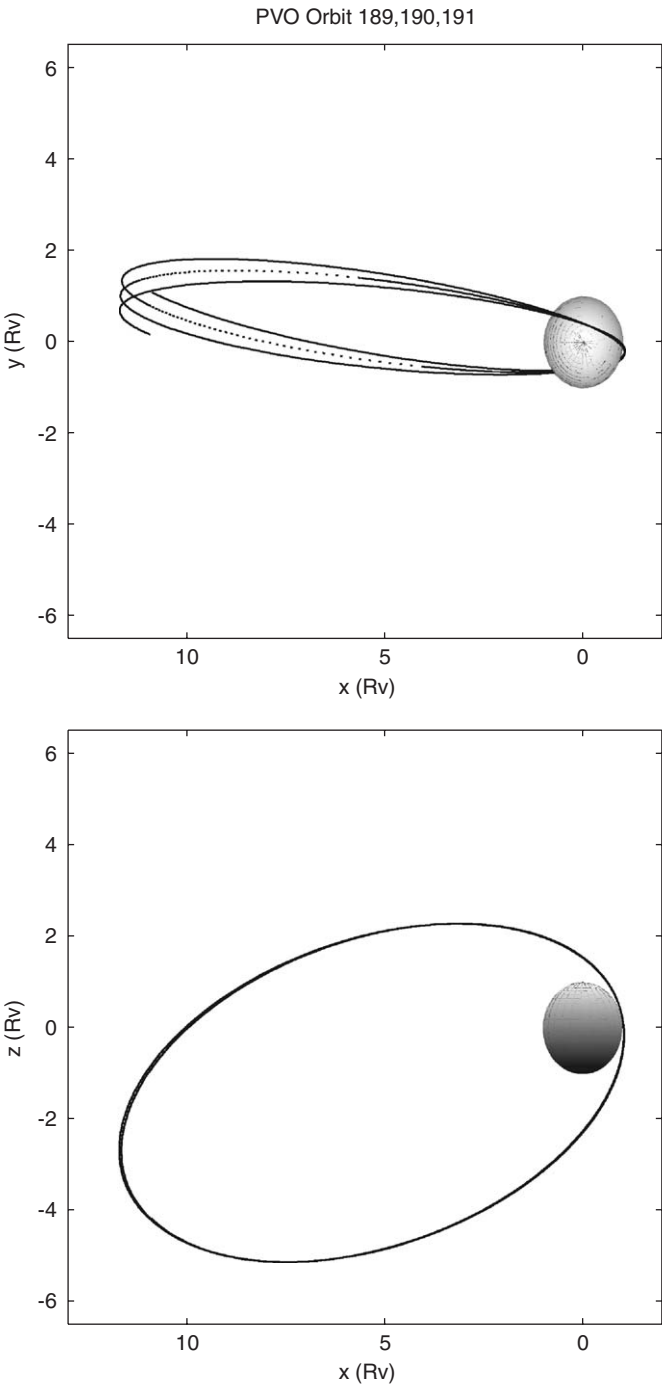

Fig. 2. Samples of PVO orbits when the local time of periapsis was optimum for wake measurements.

If the ion is created and picked up in the dayside upper atmosphere it may impact the exobase and be reabsorbed, but model estimates suggest that at least the order of ~1.e25 O^+ ions/s continue downstream and into the solar system beyond 0.73 AU (e.g. Luhmann and Bauer, 1992). Also of interest is the reabsorbed component, which may cause sputtering of additional neutral constituents (including oxygen) from the exobase (Luhmann and Kozyra, 1991). Sputtering can contribute either directly to the total oxygen loss rate, or to the neutral exospheric population available to be ionized and picked up in the solar wind. Other observations at lower ion energies have been interpreted as suggesting comparable O^+ ion escape by mechanisms such as polar wind-like outflows (Hartle and Grebowsky, 1990) and solar wind-ionosphere boundary instabilities (e.g. Brace et al., 1982), but these remain less certain and less addressable by the available observations.

Observations of escaping pickup O^+ by the PVO plasma analyzer have been described in several earlier papers. Mihalov and Barnes (1982) used the measurements to estimate the escaping fluxes. Intriligator (1989) demonstrated that in the wake the ions are asymmetrically distributed with respect to the cross-flow interplanetary magnetic field orientation, as expected for pickup of this large gyroradius (compared to the planet radius) ion species. A large (nine magnetotail pass seasons covering the years 1979 to 1984) collection of O^+ observations in the magnetotail, including their solar wind and interplanetary and local magnetic field context, were analyzed by Moore et al. (1990), who also considered the implications for atmospheric escape.

The PVO mission operated from 1978 to 1991, producing over 5000 orbits of returned and archived data. Now that the Venus Express mission carrying the ASPERA-4 ion

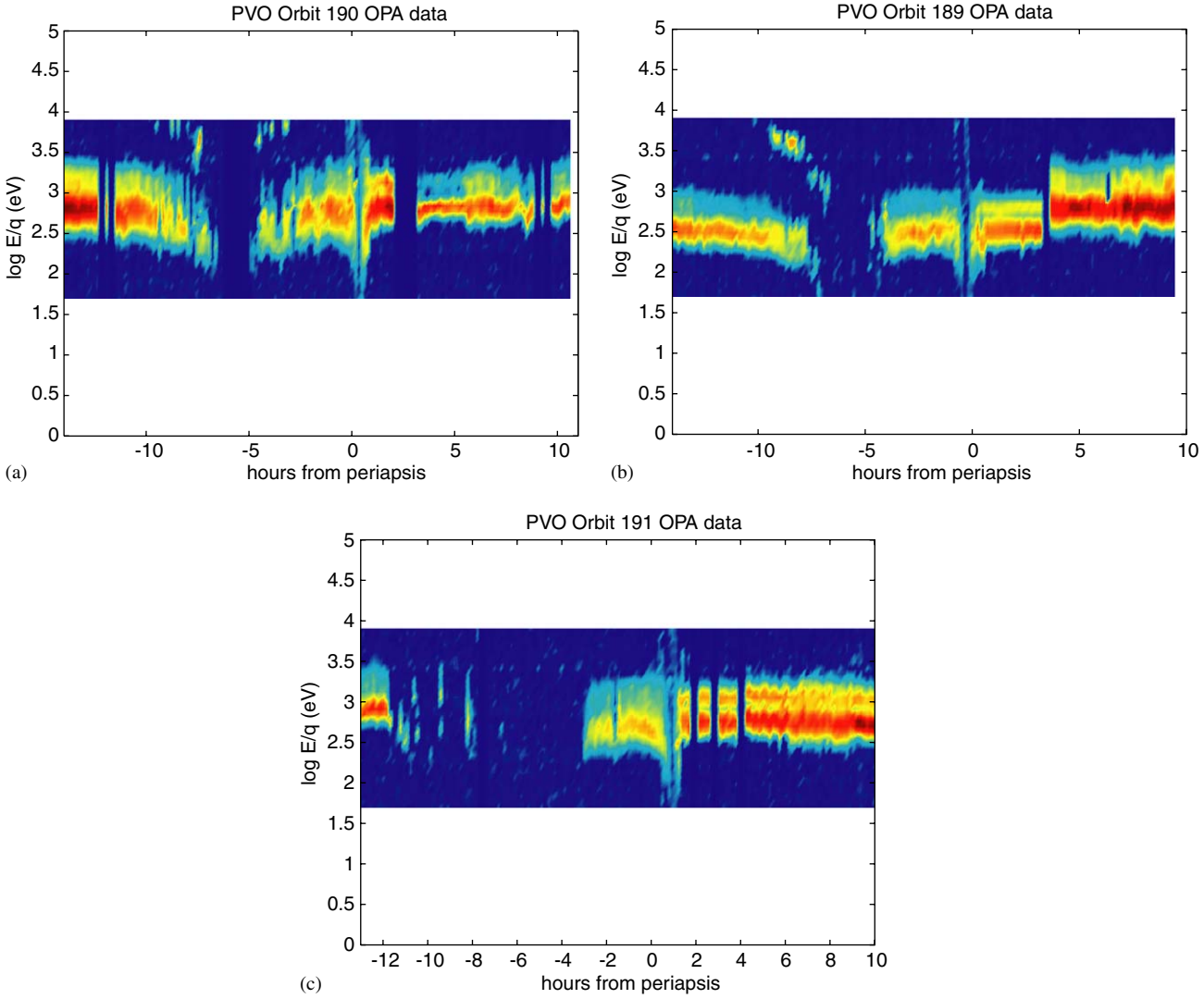

Fig. 3. Energy spectrograms obtained from the plasma analyzer data for the orbits shown in Fig. 2. The inferred O^+ is seen as the higher energy peak coexisting with the main proton peak (e.g. in (a, b)), or as single peaks in the wake proton void (e.g. in (c)). (a) PVO orbit 190; (b) PVO orbit 189; (c) PVO orbit 191.

mass spectrometer (Barabash et al., 2004) has returned to Venus, we are motivated to revisit the complete 14-year mission data set of PVO plasma analyzer O^+ observations from the perspective of what to expect. In this paper we show the statistical properties of the collected observations of ion energies and detection locations, and then use the data to construct ion spectrograms like those that will be used to interpret Venus Express observations. We then use a model of the pickup O^+ ions to compare against the PVO observations, and to anticipate the results from the broader energy and angular coverage ASPERA-4 experiment. The results illustrate how interplanetary magnetic field orientation and spacecraft orbit geometry play together to create particular perspectives on the escaping fluxes.

2. Observations

The Pioneer Venus Orbiter Plasma Analyzer (PV OPA) has been described in the literature a number of times (Intriligator et al., 1980; Mihalov and Barnes, 1982; Moore

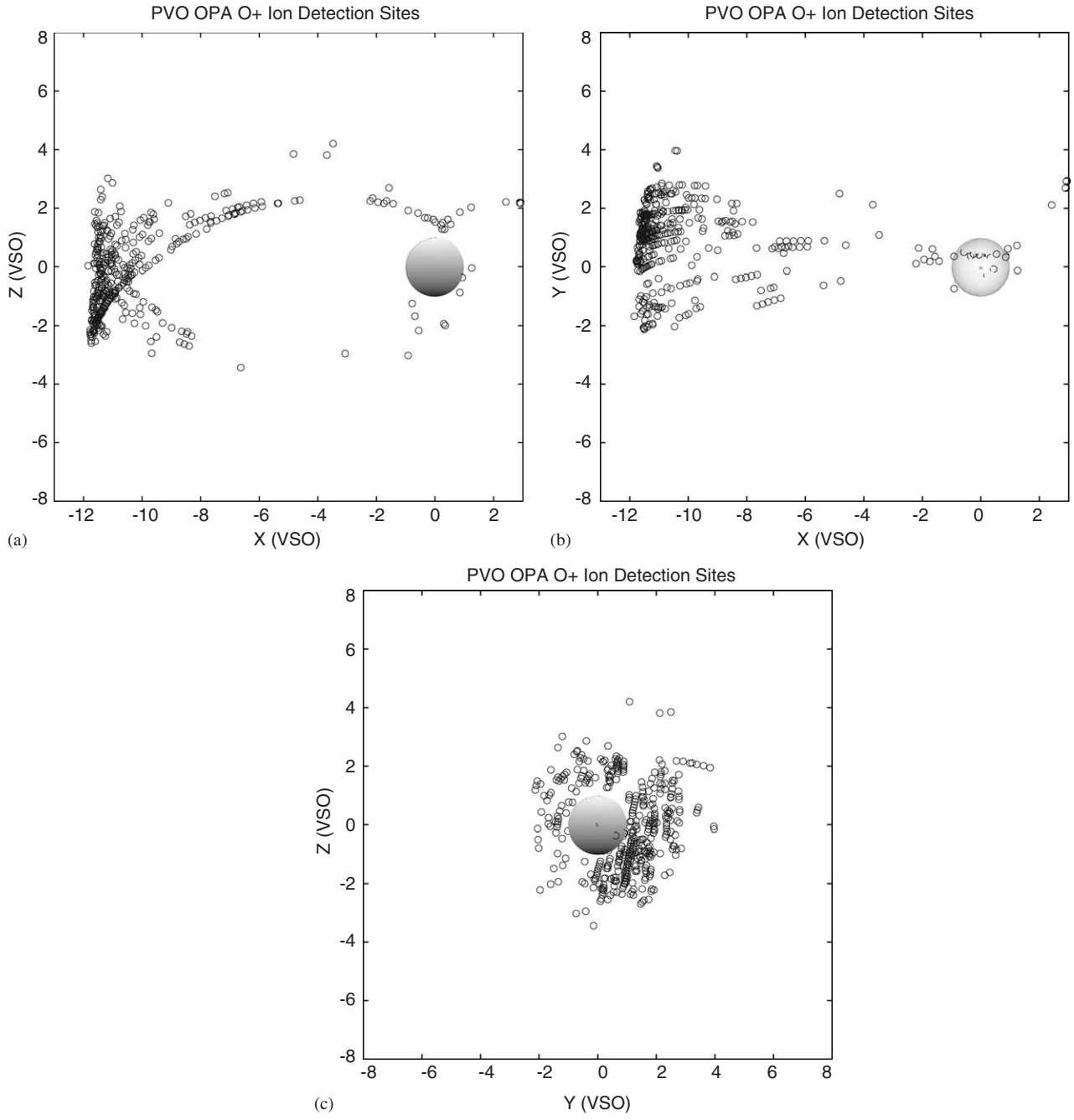

Fig. 4. Orthogonal projections of locations of measured O^+ peaks on PVO. (a) noon-midnight meridian (x(VSO)—z(VSO) plane) view; (b) view looking down on the north pole; (c) view from the Sun.

et al., 1990), and so we refer the reader to these descriptions of its design and operation. Essential features from the viewpoint of this report are the ~8 keV/q energy per charge upper limit for detection and the directional sampling scheme, allowing detection with ~15 deg. azimuthal and ~20–30° polar angle resolution with respect to the PVO spin axis. The latter enables detection of the solar wind plasma flowing anti-Sunward (e.g. at zero azimuth and 90° polar angle) upstream of the bow shock, or deflected around the Venus obstacle in the postshock sheath region, as well as the picked up O^+ ions moving at any angle with respect to the solar wind plasma flow. The time resolution for a full angle and energy scan is about 9 min. An additional limitation of the data obtained was the transmission of only that energy scan obtained in the direction of maximum flux. As a consequence, reconstruction of a full ion distribution function with angle as well as energy information is not possible, even though it was measured. This limitation implies that a significant amount of the O^+ present is missing in the data set because pickup ions often move in directions at large angles to the background solar wind flow.

O^+ ions are inferred to be present in the PV OPA energy scans when a second peak is visible at high E/q. Fig. 1, reproduced from Mihalov and Barnes (1981) illustrates this second peak in the spectrum, which on occasions contains higher fluxes than the low energy peak. However, as Moore et al. (1990) point out, the solar wind proton peak usually vanishes in the central wake. Thus wake spectra with single isolated peaks that seem contiguous with the trend followed by the high-energy peaks in adjacent energy scans where both peaks are present are also inferred to be O^+ detections. Isolated peaks in the deep wake proton void are also counted as O^+.

For the purposes of this study, energy spectrograms were created from the plasma analyzer data for each of the ~5000 PVO orbits. Sample spectrograms obtained when PVO passed through the Venus wake at apoapsis on the orbits in Fig. 2, are shown in Figs. 3a–c. These ~24 h single orbit spectrograms were visually scanned for the second higher energy peaks expected for O^+, and for single peaks in the deep wake where the proton peak has vanished. The appearance of the oxygen peaks differs from orbit to orbit, even for the same orbital sampling geometry, due to the variability of the solar wind and especially the cross-flow interplanetary magnetic field orientation. Later we use a model of the pickup ions to illustrate the latter effect. The locations and energy per charge (E/q) values for each of these peaks were recorded. Periapsis traveled around the planet once a Venus year (~224 Earth days) so that apoapsis was often far outside the wake. Nevertheless, O^+ detections made away from apoapsis tell us about the broader spatial distribution of the picked-up O^+. The orbit also evolved during the mission, with periapsis rising and apoapsis decreasing in altitude. A total of 427 O^+ peak detections obtained from orbit 8 through orbit 4687 were recorded in our survey, compared to the 296 detections analyzed by Moore et al. (1990).

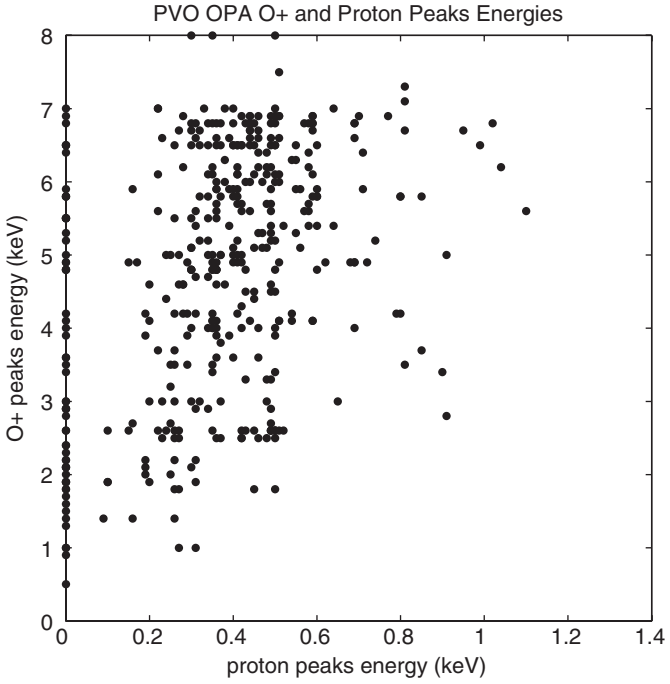

Fig. 5. Relative E/q values of proton peaks and oxygen peaks in the OPA E/Q spectra. A zero proton peak energy implies the presence of only an inferred O^+ peak, based on its proximity to other O^+ peaks or location in the wake proton void. PV OPA has an ~8 keV detector E/q limit for O^+ detection.

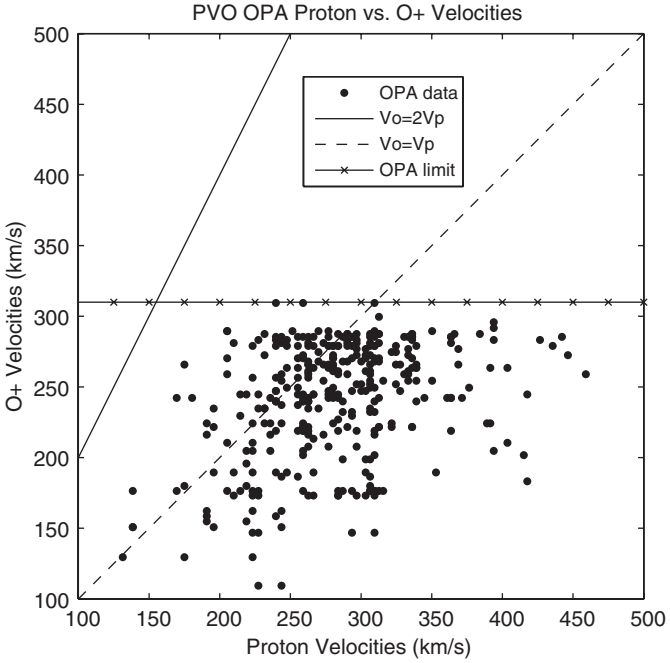

Fig. 6. Relative velocities of protons and inferred O^+, showing a trend toward similar velocities in the Venus environment. The PV OPA cannot detect O^+ moving at speeds greater than ~310 km/s, equivalent to ~8 keV energy.

The cross-flow interplanetary magnetic field (IMF) orientation is expected to create changing asymmetries in the O^+ spatial distribution due to the large gyroradii of the picked-up O^+ ions (~.5–1 Rv (Venus radii)) relative to the size of the planet and the solar wind interaction region. As the direction of the IMF draped around Venus is typically eastward or westward, the convection electric field $E = -VXB$ (where V is the solar wind plasma velocity and B the local magnetic field) produces pickup ion trajectories that are initially either northward or southward as well as anti-Sunward. If the ion trajectory does not intersect the exobase at a few hundred kilometers altitude, the trajectory continues down the wake in a hopping cycloidal motion. Thus, near the planet terminator and in the near-planet wake one should observe that the O^+ detection locations are organized into northern or southern spatial clusters as observed by Intriligator et al. (1987) and Moore et al. (1990). To better organize and interpret the collected O^+ observations from PV OPA, the PV magnetometer data (Russell et al., 1980) were used to determine the magnetic fields at the times of the scans showing O^+ peaks. We note that Moore et al. recognized that the field perpendicular to the Venus–Sun line at the O^+ detection point also reflects the upstream conditions at the time of the pickup, allowing one to estimate its orientation without an upstream spacecraft monitor to a good approximation.

3. Statistical analyses of O^+ positions and energies

The locations of the collected O^+ detections relative to Venus are illustrated in Fig. 4a–c. These are plotted in a Venus Solar Orbital (VSO) coordinate system in which the X-axis points toward the Sun, Y-points along the planet's orbit in the direction opposite planetary motion, and Z-points northward to complete the right-handed set. VSO is the Venus counterpart of the GSE system at Earth. These plots show the sampling bias introduced by the PVO orbit geometry, but it is nevertheless clear that most of the O^+ detections are found within ~3 Rv of the Venus–Sun line in the wake. The preference for the $+Y$ direction is consistent with the expected aberration of the wake due to Venus' orbital motion through the radially flowing solar wind.

The energies at which the inferred O^+ ions were detected are compared with their accompanying proton peak energies in Fig. 5. Here, zero proton peak energy identifies those inferred O^+ detections not accompanied by a proton peak in the same spectrum. At 16 times the proton mass, comoving O^+ ions will have 16 times the proton energies. The statistics suggest the detected O^+ peaks are at roughly these energies up to the 8 keV limit of the PVO plasma analyzer. O^+ moving at greater than ~310 km/s will be outside of this range. Thus significant numbers of detections were likely missed in

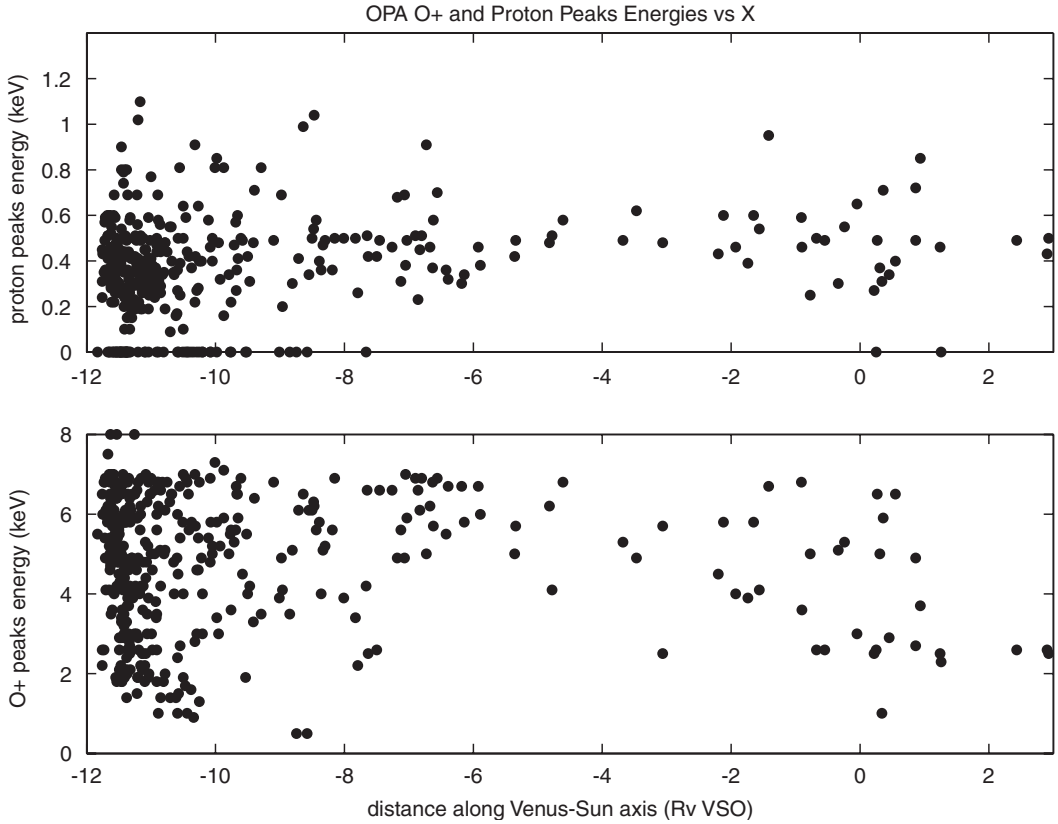

Fig. 7. Energies of proton and inferred O^+ peaks show no trends with down-tail distance. PV OPA has an ~8 keV detector E/q limit for O^+ detection.

the upstream solar wind, outer magnetosheath, and distant wake where the solar wind plasma often moves at speeds of 350 to over 600 km/s. This limitation is hinted at by Fig. 6, which shows the implied velocities of the detected O^+ plotted against the accompanying proton peak velocities. Also shown in this figure is the expected velocity limit for pickup ions in perpendicular flows and magnetic fields of twice the background (proton) flow speed. The apparent clustering about the slope one line suggests that either the ions are picked up where the angles between the solar wind flow and magnetic field are intermediate, or evolution of the distribution function has accompanied their propagation into the wake. Fig. 7, which shows the energies versus down-tail (-X) distance, shows little evidence of a consistent evolutionary trend in the energy as the ions move downstream to ~12 Rv.

The previously found control of the pickup ion detection locations by the solar wind electric field, mentioned above, is confirmed by the rotation of the O^+ detection locations about the Sun–Venus line to coalign the perpendicular local magnetic field orientations.

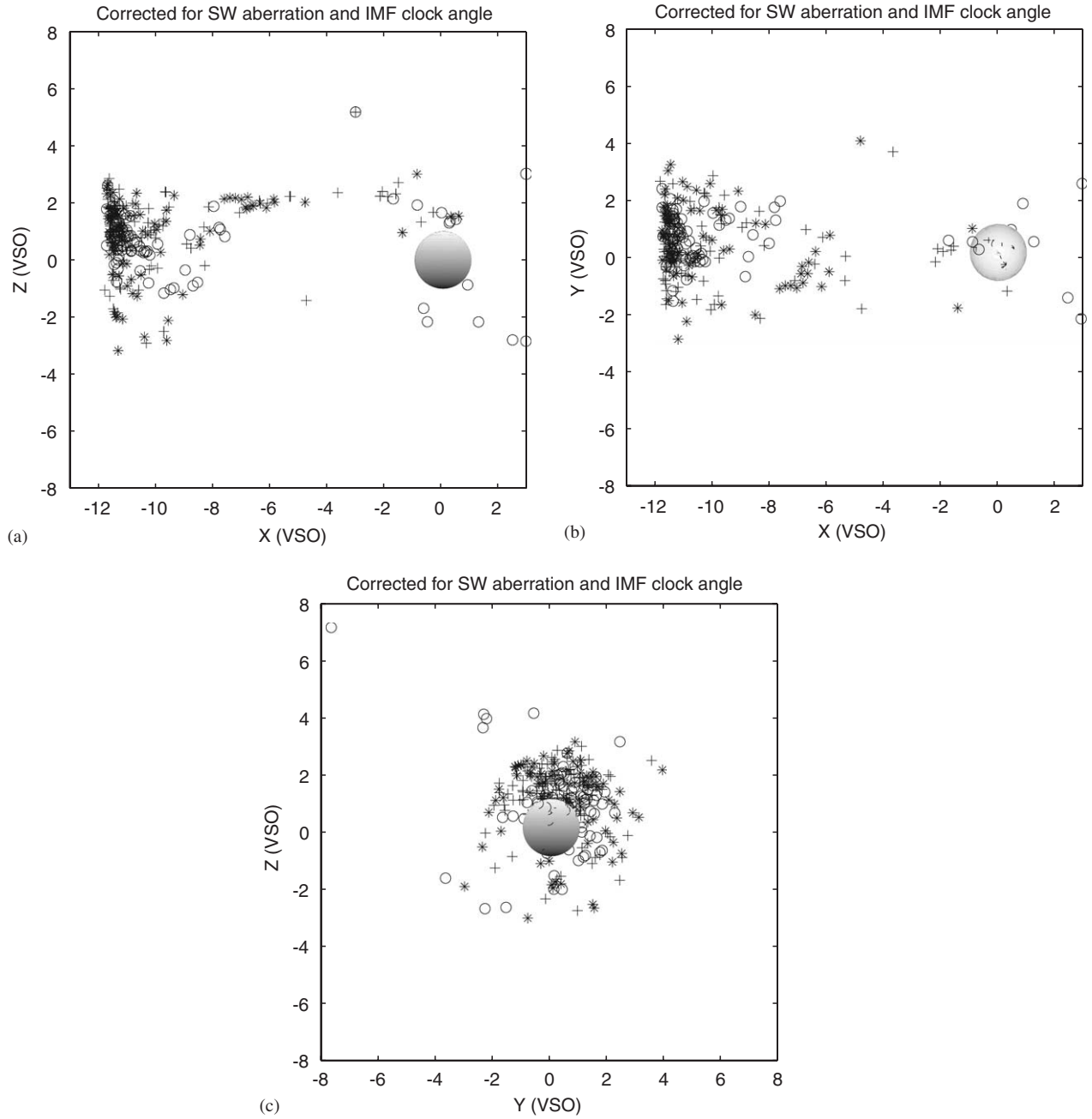

Fig. 8. Views of locations of the above O^+ peaks, rotated according to the prevailing IMF clock angle and sorted by energy (low [open circles] is $E<4$ keV, medium [plus symbols] is $E=4-6$ keV, high [asterisks] is >6 keV).

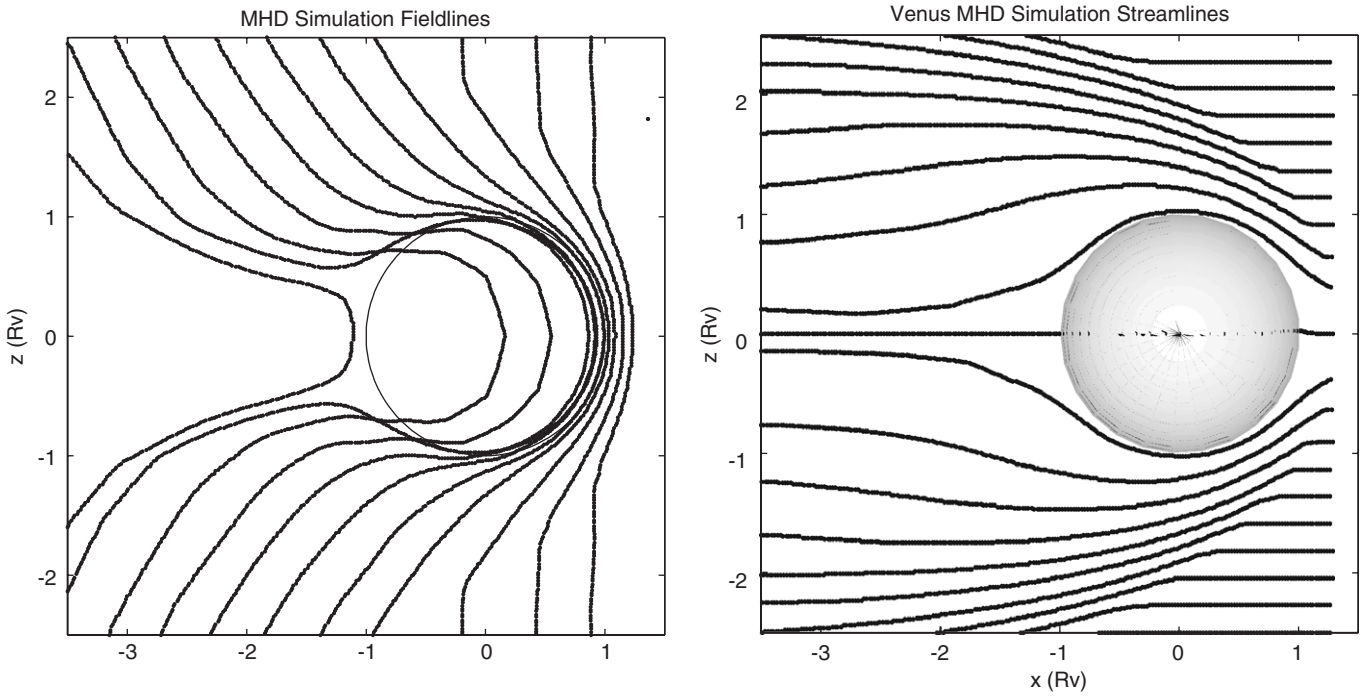

Fig. 9. Basic attributes of the MHD model of the Venus-solar wind interaction used in the present study. Shown are draped field lines in the plane of the IMF and streamlines.

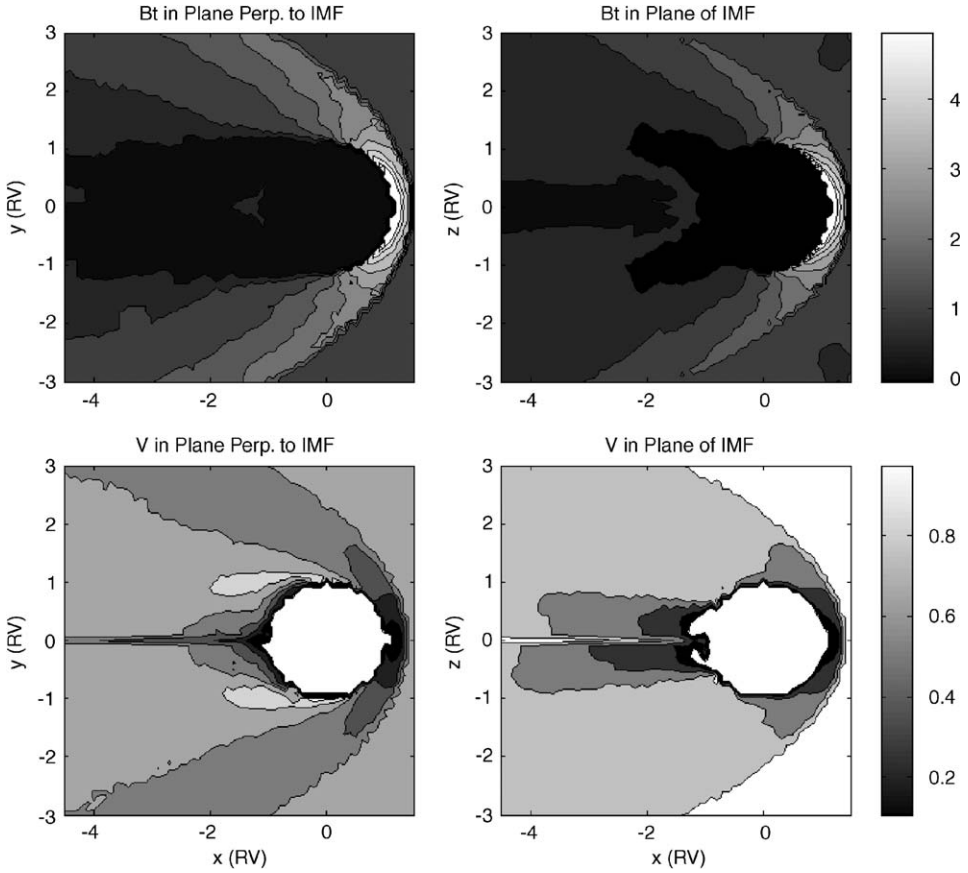

Fig. 10. Color contours of field and flow velocity magnitude in the plane of the IMF and the perpendicular plane. The contour values are normalized to upstream values. These parameters are used to compute the $E = -VXB$ and B fields used in the test particle model.

Figs. 8a–c show plots corresponding to Figs. 4a–c with both this rotation and a correction for average tail aberration applied. Cases where the magnetic field was difficult to characterize due to its variability are omitted. The rotation of the positions corresponds to pointing all of the local perpendicular magnetic fields in the $+Y$ direction. As previously found, the resulting clustering of the detections in the $+Z$ hemisphere in Fig. 8c is clear evidence of both the ion pickup process and the effect of the finite O^+ gyroradius effect on the pickup ion distribution at these energies. To search for any energy dependence in these distributions, the points in Fig. 8a–c distinguish three energy ranges derived from the spectral peaks. Those designated as low energies occur at <4 keV, medium falls between 4 and 6 keV, and high is between 6 and the 8 keV limit. While no obvious patterns are seen in Fig. 8a–c related to this energy separation, the distinctions between these ranges is not great enough to rule out such a trend over a broader range of sensitivity and with wider spatial sampling in Z. Moreover, very low-energy O^+ may be indistinguishably merged with the proton peaks in this data set, while the 8 keV upper energy limit is well below the ~60–80 keV pickup O^+ ion energies that could result from high altitude dayside pickup in a fast solar wind stream.

4. Model comparisons

In order to gain insight on the O^+ distribution both inferred by and missing from the PVO observations due to energy, composition, angular, and spatial sampling biases, we apply a test particle model of Venus pickup ions based on fields derived from a previously described global MHD simulation of the Venus-solar wind interaction (Kallio et al., 1998). The basic attributes of this model, which agrees well with the PVO magnetometer observations of the bow shock and sheath region, are illustrated in Figs. 9 and 10. Fig. 9 shows the classical picture of the interplanetary magnetic field lines projected into the plane containing the interplanetary magnetic field (IMF) and the solar wind flow streamlines The field lines are draped over the conducting spherical obstacle to the solar wind flow representing the Venus ionosphere. Fig. 10 shows contours of the field magnitude and velocity in planes perpendicular and parallel to the IMF. An advantage of using such an MHD model is that it includes the realistic asymmetries resulting from the compression and draping of the IMF. The interplanetary conditions chosen for this simulation are typical of those at Venus, with a solar wind velocity and density of 400 km/s and 18 cm^{-3}, respectively. The 14 nT interplanetary field was presumed to be perpendicular to the upstream flow. Thus we do not include effects associated with the ~40° nominal Parker spiral angle at 0.73 AU, which are secondary to IMF "clock angle" effects in controlling pickup ions near Venus. Most of the time the perpendicular interplanetary field lies near the planet's orbital plane, in the $+Y$ or $-Y$ direction, depending on the solar and coronal magnetic field. We also do not include the effects of time-varying solar wind conditions, instead making use of what can be considered a typical set of conditions.

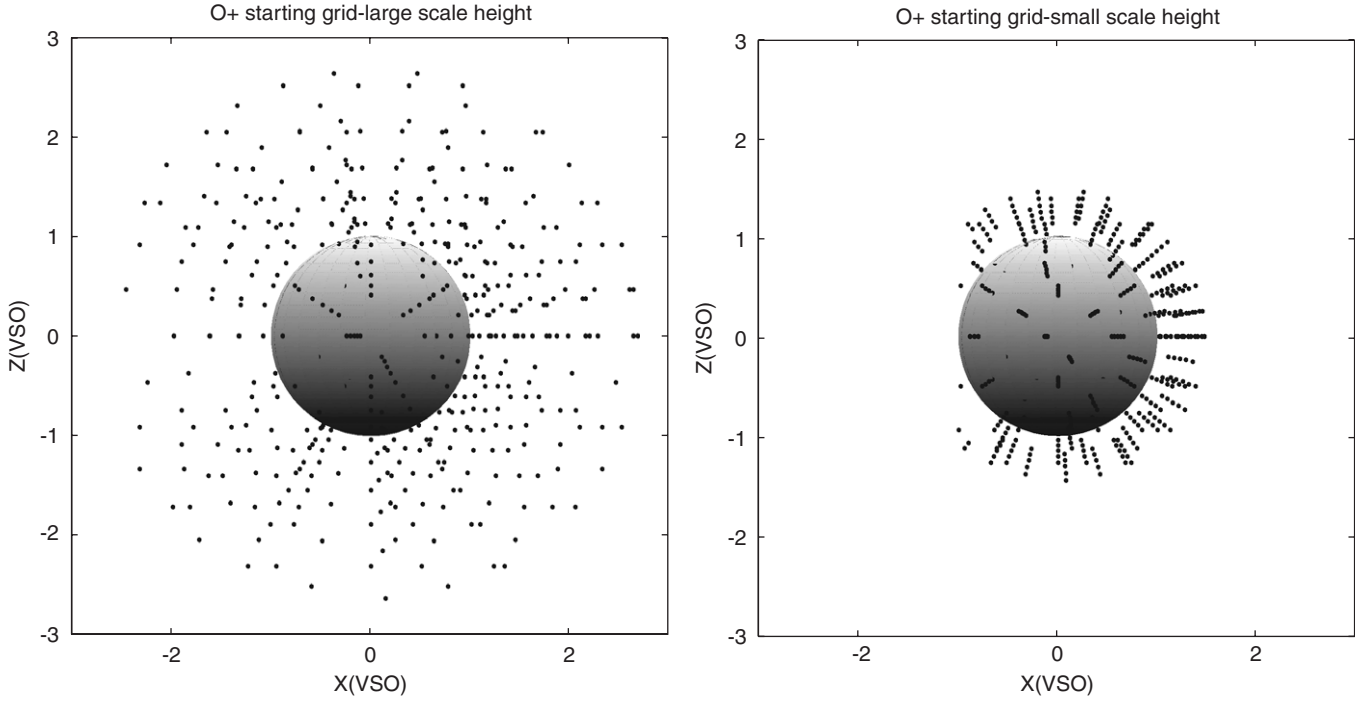

Fig. 11. Illustration of the two different exponential launch point grids used in the test particle calculations to illustrate effects of both large and small scale heights of the atmospheric source of O^+ ions.

We inject O^+ test particles into this model with initially zero velocities at starting points representing the upper atmosphere density distribution. For test purposes we investigate two different effective scale heights as shown in Fig. 11. These approximately represent the two basic components of the upper atmosphere of Venus that is exposed to the solar wind (e.g. see Kallio et al., 1998 Fig. 2). Both of these starting point grids contain ~500 locations scattered approximately uniformly over spheres logarithmically spaced in radius, but one is distributed within 1.2–1.5 Rv and the other within 1.2–2.7 Rv. To mimic an expected night-side falloff in the exosphere

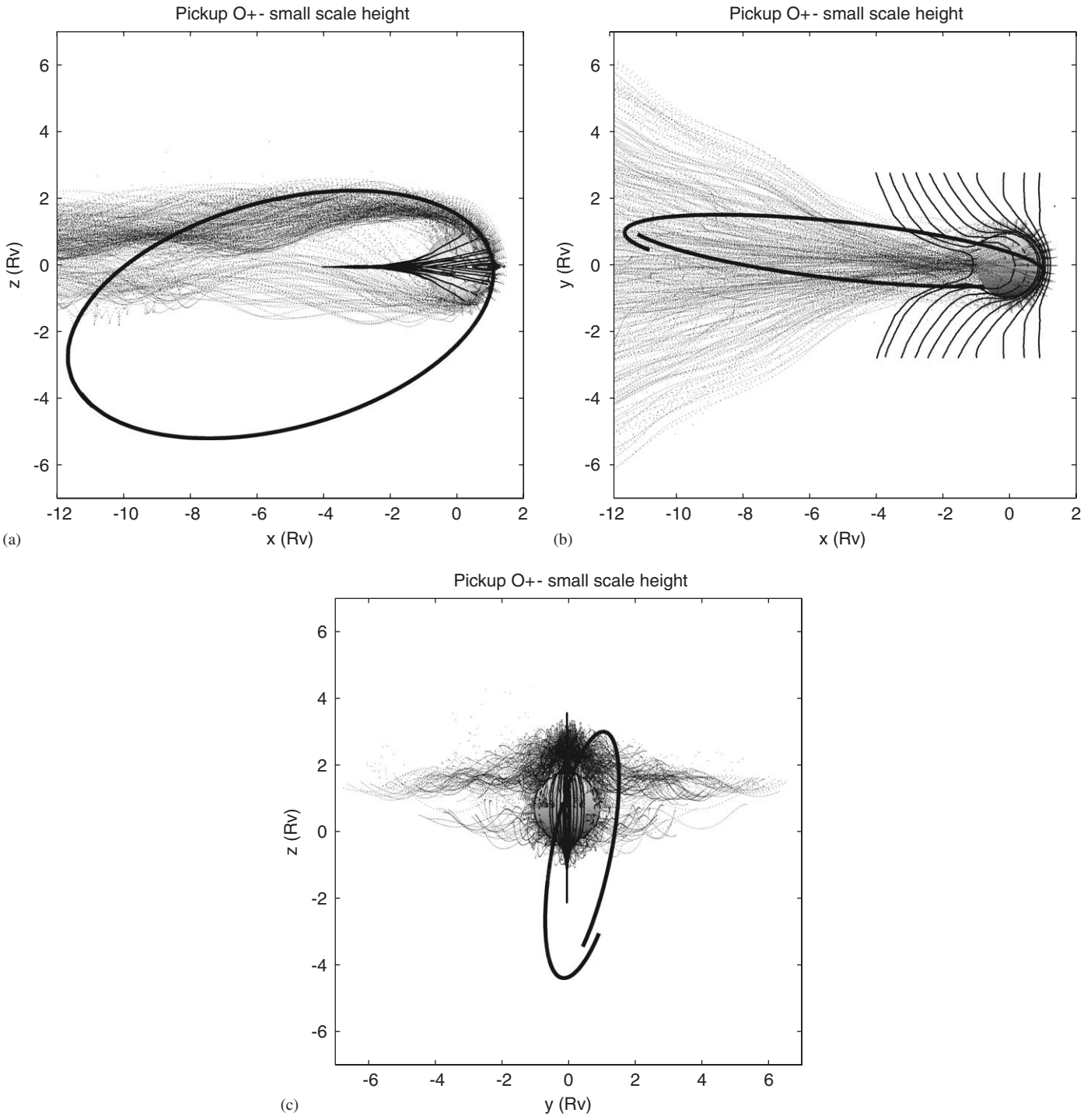

Fig. 12. Orthogonal views of trajectories of ~500 O^+ pickup ion test particles launched in the MHD model fields using the small-scale height starting grid. A sample PVO Orbit with optimum O^+ sampling orientation (Orbit 190) is superposed.

density and O^+ production rate, starting points in the optical wake were excluded.

The trajectories of the picked up O^+ test particles for the two starting grids calculated with the model interplanetary field in the positive Y direction are illustrated in Figs. 12 and 13. A sample PVO orbit is superposed to illustrate the optimum sampling geometry when the apoapsis is in the wake. In Fig. 14 the interplanetary field direction has been reversed to suggest the sensitivity of the observations to its direction. Note that for the small scale height starting grid the trajectories in the view from the Sun fan out into an ion wake elongated along the field direction (as also shown in Moore et al., 1991), while for the more extended exosphere grid they are more symmetrically distributed with respect to the wake axis, with a shift north corresponding to the solar wind convection electric

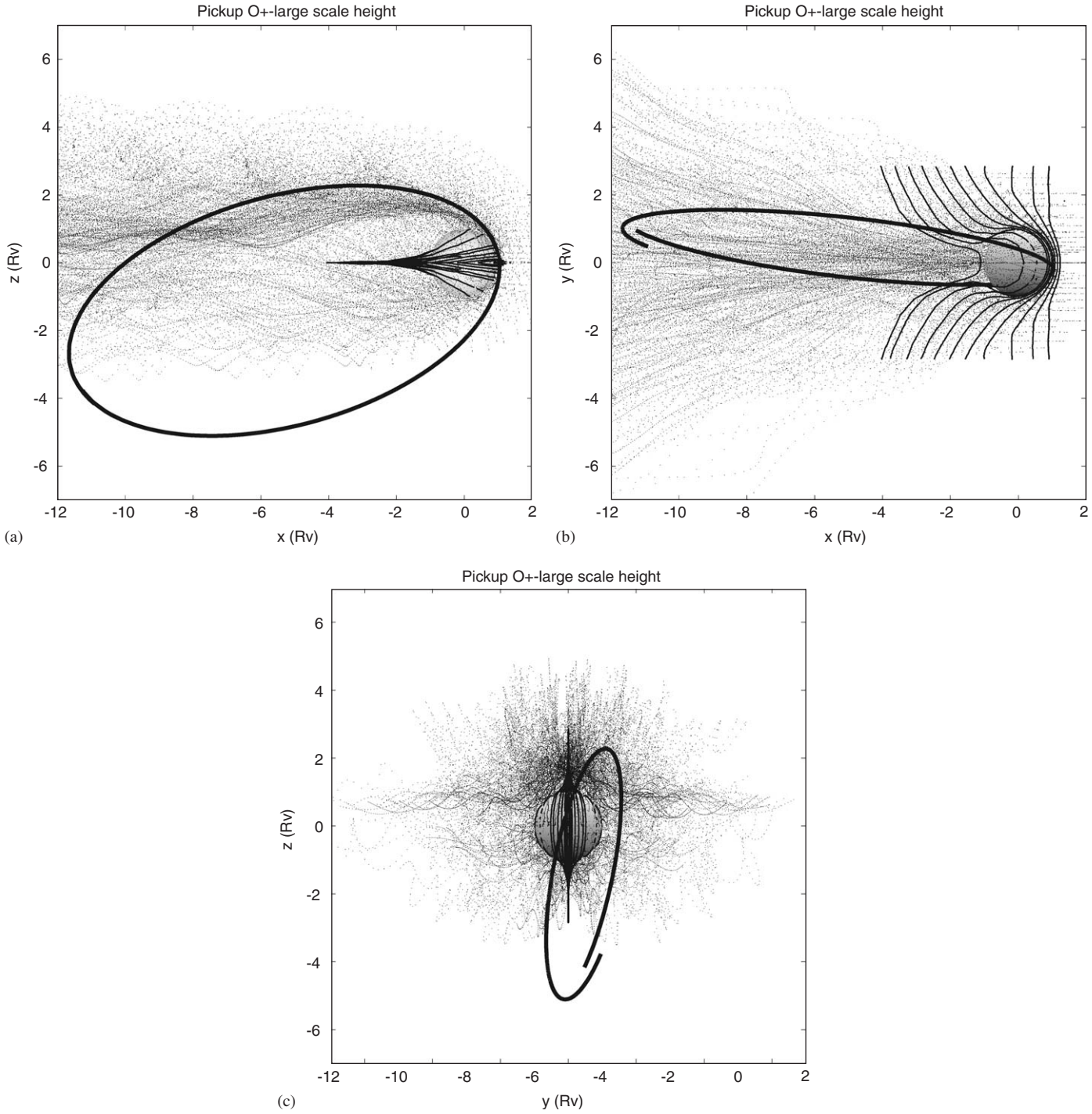

Fig. 13. Same as Fig. 12 but for the large-scale height-starting grid.

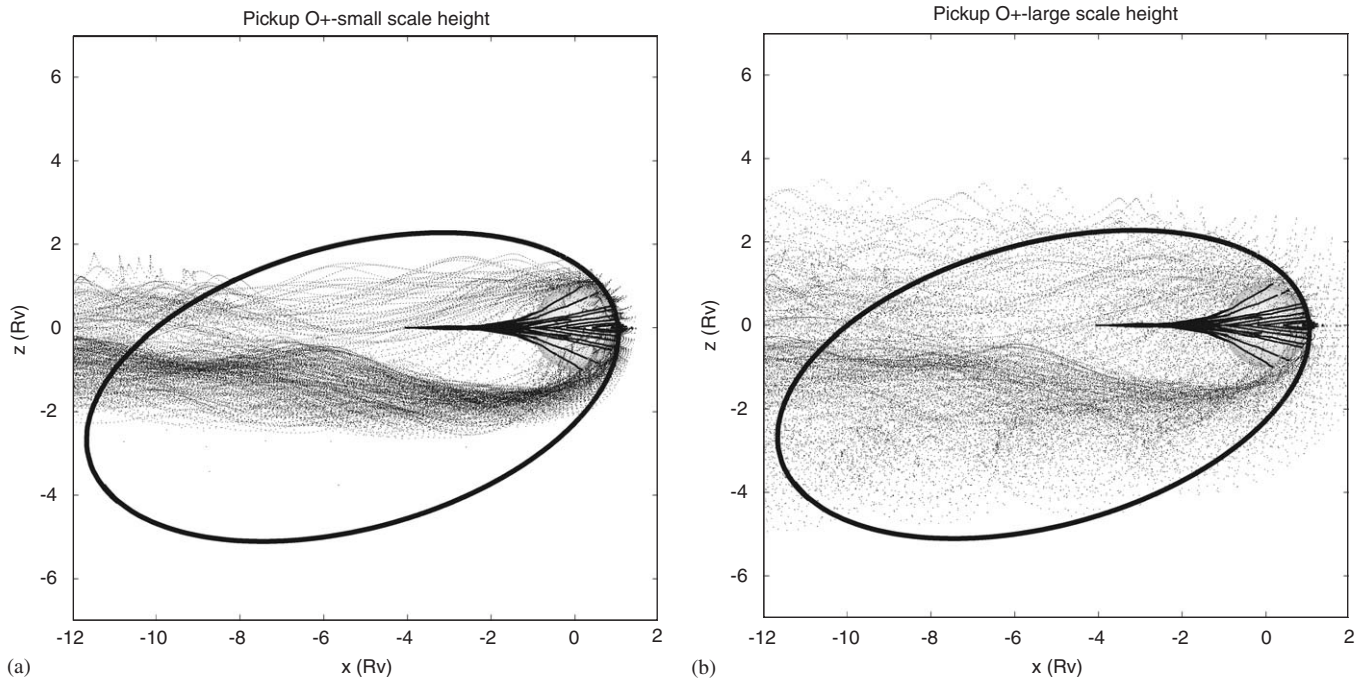

Fig. 14. A reversed IMF polarity case is also shown for comparison with Fig. 12. Both the orbit and the IMF orientation are important in determining what is observed.

field effect mentioned earlier. Analysis of the energies at specific down-tail cross sections (not shown) indicate that, as in the observations (Fig. 8), the O^+ energies show no clear spatial segregation. The reason is that the energies oscillate with large spatial scales, and are out of phase for different particles depending on their location of initial pickup.

We next calculate simulated O^+ energy spectrograms analogous to those in Figs. 3a–c. In this case we do not have the complication of the solar wind proton contributions, and so can isolate the O^+ information. These represent what might have been seen had the PVO plasma analyzer had full energy coverage from 0 to 500 keV and the ability to separate the O^+ pickup ions from the protons. PVO Orbit 190 (see Fig. 2) was used to represent the sampling geometry common to the observed spectrogram examples. It was effectively flown through the test particle cloud, such that the numbers of particles and their energies within a ~1 Rv sphere about each orbit sampling point were used to construct the statistical information for the simulated spectrogram. No angular or detector field of view restrictions were imposed. This coarse sampling is relatively consistent with the ~9 min sampling cycle of the PVO plasma analyzer, and with the large pickup O^+ gyroradius scales. The orientation of the IMF was also reversed in order to gain insight into the effects of IMF rotation on the appearance of the spectrogram.

Figs. 15a–d show the results of the simulated spectrogram analyses. Figs. 15a and b compare results for a +By IMF for the small- and large-scale height sources, respectively. Figs. 15c and d show the same plots for -By IMF. When compared with Figs. 3a–c, the information missing in the PVO data set because of its lack of composition separation and its limited energy and angle ranges can be appreciated. At the same time, one can see features in both the test particle simulation results and the observations that agree in some respects but also raise questions. In particular, the model suggests that the near-periapsis O^+ features should be more prominent at higher energies than they appear to be. This could be the result of mass loading in the pickup ion region at low altitude that is not accounted for in the MHD model used here, or occurrence of the higher energies in an angular window not coincident with the maximum flux of the proton flow. Mass loading would make the pickup velocities lower near the planet, and thus more difficult to distinguish from the heated solar wind protons in the sheath. (We elected not to use the mass-loaded MHD model described in Kallio et al. (1998) in order to obtain the most basic result.) Pickup ions also initially move perpendicular to the background magnetic field which is perpendicular to the solar wind proton flow. Another finding suggested by these qualitative comparisons is that the observations better resemble the smaller scale height starting grid model. Additionally, in the small-scale height case the time of the wake O^+ detection relative to periapsis time is significantly shifted by the IMF orientation change. The picked-up O^+ observations can thus be used as a means of inferring the scale height of the source region, even when they are obtained far from the planet.

One additional analysis that can be carried out with the test particle model results is the angular distribution of the

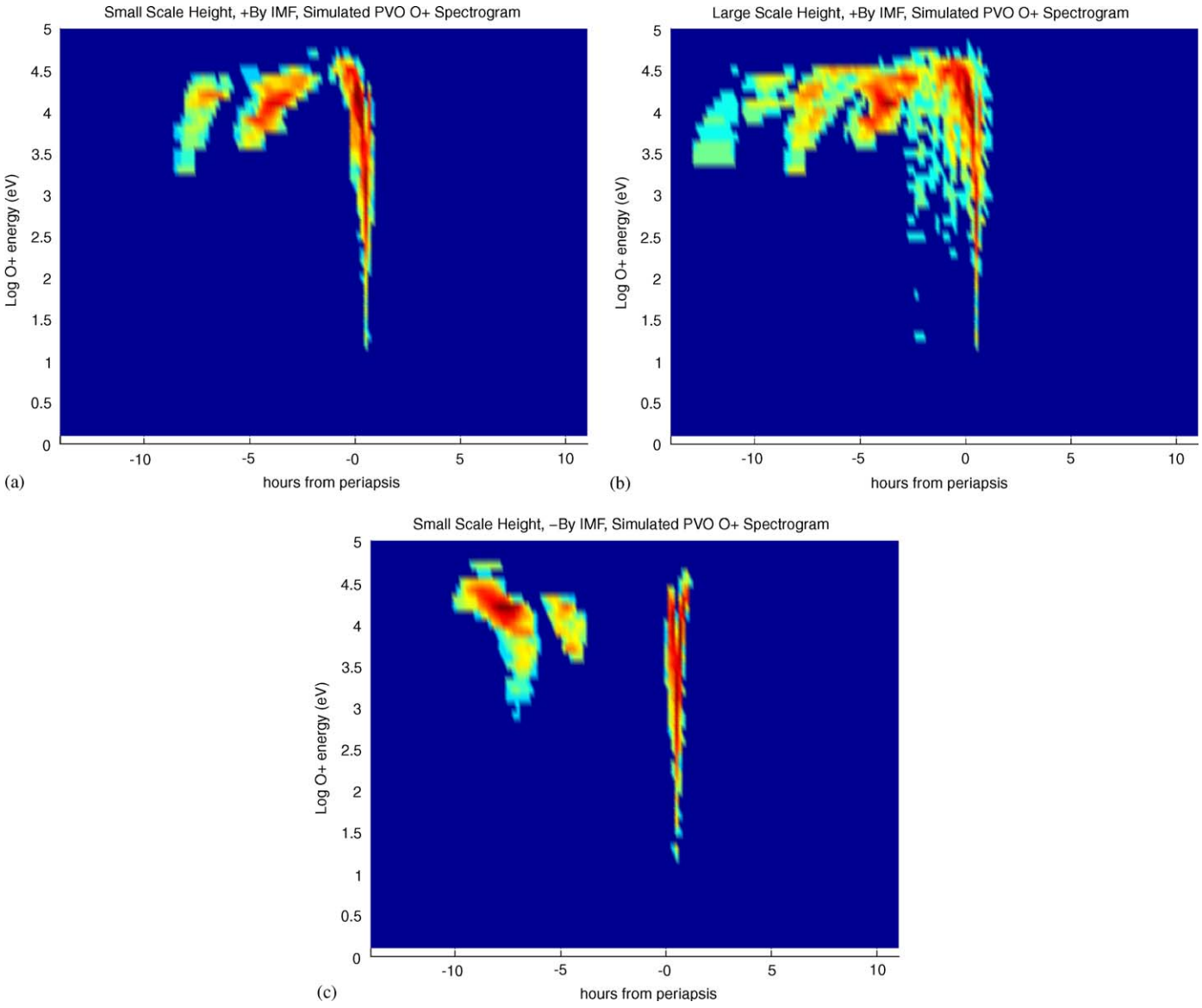

Fig. 15. (a) Simulated O^+ Energy spectrograms computed from the statistics of the test particles for the small-scale height, + By IMF case, along the PVO orbit shown in Fig. 12. The statistics contributing to each E/q spectrum are derived from particles passing within 1 Rv of each orbit sampling point. This relatively course sampling is consistent with the ~9 min sampling by the OPA, and with the large O^+ ion gyroradius scales. No angular restrictions were imposed on the sampled particles, thus these spectrograms represent what might be observed with an omnidirectional detector. (b) Same as (a) but for the large scale height source. (c) Same as (a) but for -By IMF. (d) Same as (b) but for -By IMF.

pickup ions. With the caveat that we have assumed a scatter-free environment, we computed the pitch angles for the particles in the sampling spheres from the local fields at the particle sites, and sorted them into ~3.5° bins. In Fig. 16, we plot the resulting time sequence of pitch angle distributions along the orbit as a spectrogram-like counterpart for the model example in Fig. 15a (small exospheric scale height, + By IMF case). The results show that as expected, the initial pickup where the field is highly draped around the dayside of the planetary obstacle is at 90° pitch angles. In the wake, the O^+ ions travel more along the field direction. The extent to which this behavior may have biased the PVO plasma analyzer observations, due to its telemetered data strategy, is not clear. However, this display suggests another useful data analysis and model comparison tool.

5. Implications for ASPERA-4

The above results suggest the extent to which ASPERA-4 on Venus Express (Barabash et al., 2004), with its energy range of ~0–40 keV, scanning field of view, and ability to separate ion masses, will greatly improve our view of the pickup ion environment

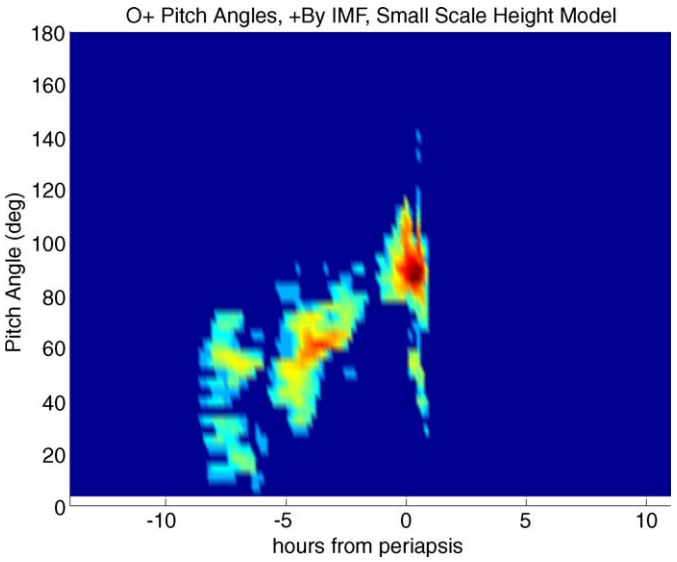

Fig. 16. Spectrogram-like display showing the time series of test particle model pitch angle distributions for the case displayed in Fig. 15a.

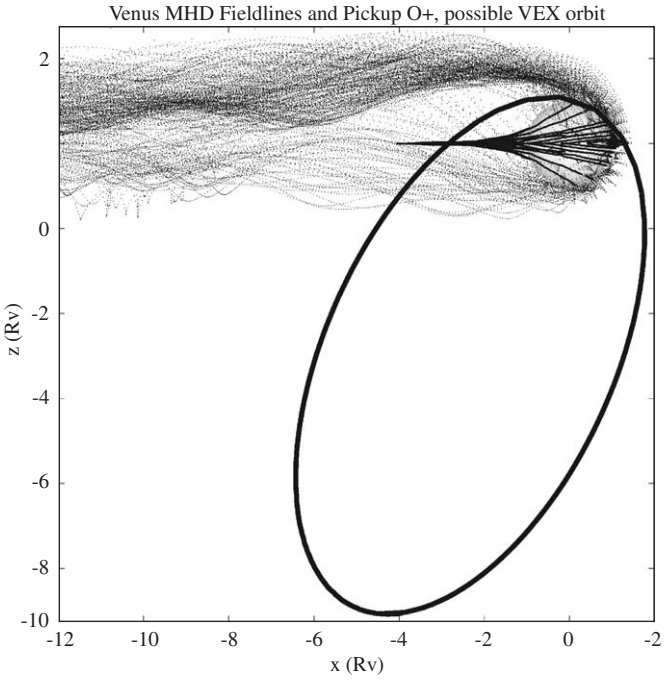

Fig. 17. Illustration of the proposed Venus Express orbit with its periapsis at ~65 deg *N* latitude, relative to the test particle trajectories in Fig. 12a. The more restricted sampling of the pickup ion wake is advantageous for near-planet pickup studies but misses many of the ion wake attributes.

around Venus. However, careful consideration needs to be given to the operating plan as far as orbital geometry is concerned. The currently planned orbit is similar to that of PVO, but with periapsis at ~65° N Latitude and ~250 km altitude, compared to PVO's 15° N Latitude initial periapsis with nominal ~160 km altitude. The sampling of the pickup ion cloud in an orbit with this geometry is suggested in Fig. 17. The related simulated O^+ spectrograms are shown in Figs. 18a and b for the + By IMF and - By IMF cases. Unless the orbit is allowed to evolve so that periapsis drifts to lower altitudes, the ion wake measurements will be limited to within about 4 Rv. On the one hand, this inner and middle wake region was not covered by PVO observations due to the orbital sampling bias, so that Venus Express will fill this observational gap. On the other hand, a fixed high periapsis latitude orbit will miss the opportunity to add the compositional and energy coverage information potentially available from apoapsis wake observations.

6. Summary

The collected O^+ observations from the Pioneer Venus Orbiter plasma analyzer, covering over a decade, have been presented above to show the state of O^+ pickup ion observations at Venus prior to Venus Express. The observations are generally consistent with test particle models of O^+ pickup ions launched in the flows and magnetic fields described by the results of an MHD simulation of the solar wind interaction. Interplanetary magnetic field control of the observed O^+ spatial distributions are clearly indicated by both the statistical patterns of the locations of O^+ detections and by the different appearances of O^+ energy spectrograms obtained over nearly the same orbital trajectories. The observations further suggest the main source of the observed pickup ions (at energies $\leqslant$ 8 keV) is probably within a Venus radius of the surface. Comparisons of simulated energy spectrograms from the test particle model with examples of observed spectrograms indicate how much we still have to learn about pickup ions at Venus. Many of the pickup ions are inferred to be out of range of the PVO plasma analyzer energy and/or angular response. Similarly, the O^+ cannot be distinguished from the solar wind protons when the energy spectra significantly overlap, making low energy pickup O^+ detection difficult. Still, the PVO results and the models provide a tantalizing glimpse of what remains to be accomplished observationally in the quest for understanding atmosphere escape from Venus.

Acknowledgments

The PVO plasma analyzer data were made available to us by John Mihalov of NASA Ames Research Center. We are grateful to the Ames plasma analyzer team, including Aaron Barnes, for their assistance. UCLA students Sean Kilpatrick surveyed the 5000+ orbits of PVO plasma analyzer data for O^+ events, and Tamitha Mulligan assisted in the analysis of the magnetic fields during the events. This study would not have been possible without

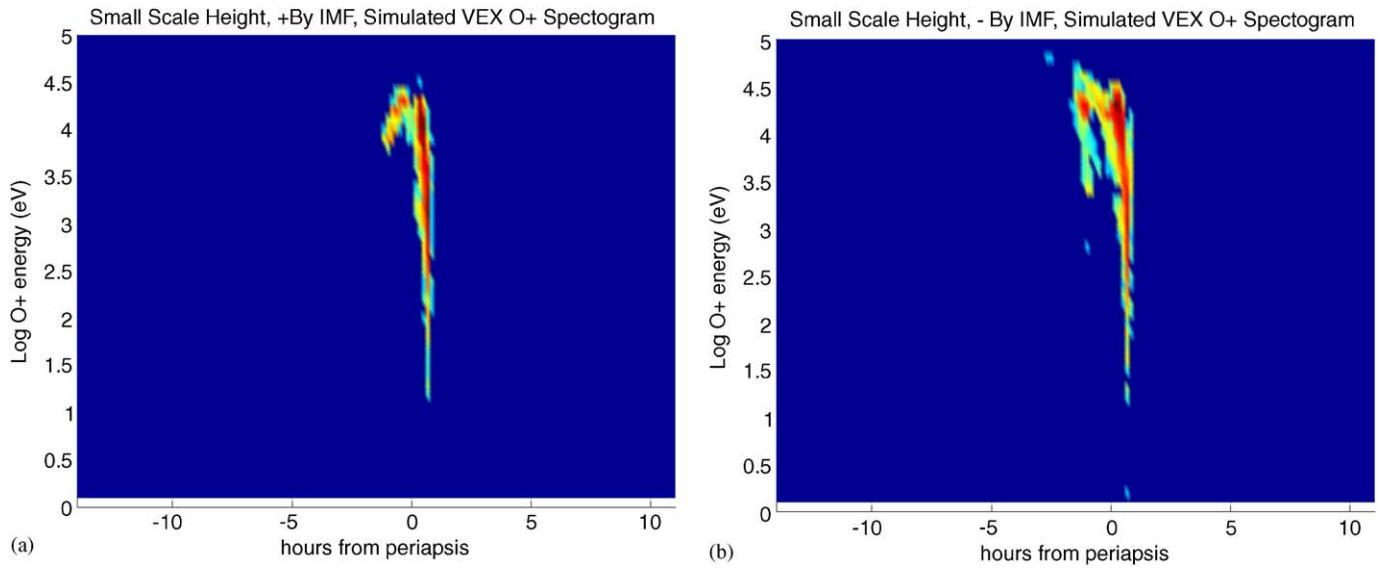

Fig. 18. Simulated O^+ spectrograms obtained for the proposed Venus Express orbit in the previous figure. (a) Small source scale height, +By IMF. (b) −By IMF case.

their contributions. This work was supported by previous grants from NASA's Planetary Atmospheres Program and the PVO Project.

References

Barabash, S., Lundin, R., Andersson, H., Gimholt, J., Holmström, M., Norberg, O., Yamauchi, M., Asamura, K., Coates, A.J., Linder, D.R., Kataria, D.O., Curtis, C.C., Hsieh, K.C., Sandel, B.R., Fedorov, A., Grigoriev, A., Budnik, E., Grande, M., Carter, M., Reading, D.H., Koskinen, H., Kallio, E., Riihela, P., Säles, T., Kozyra, J., Krupp, N., Livis, S., Woch, J., Luhmann, J., McKenna-Lawlor, S., Orsini, S., Cerulli-Irelli, R., Mura, A., Milillo, A., Roelof, E., Williams, D., Sauvaud, J.-A., Thocaven, J.-J., Winningham, D., Frahm, R., Scherrer, J., Sharber, J., Wurz, P., Bochsler, P., 2004. ASPERA-3: analyzer of space plasmas and energetic ions for Mars. In: Wilson, A. (Ed.), Mars Express: The Scientific Payload, ESA-SP-1240, ESA Publications Division, Noordwijk, The Netherlands, pp. 121–139.

Brace, L.H., Theis, R.F., Hoegy, W.R., 1982. Plasma clouds above the ionopause of Venus and their implications. Planetary and Space Science 30 (1), 29–37.

Chamberlain, J.W., Hunten, D.M., 1987. Theory of Planetary Atmospheres: An Introduction to Their Physics and Chemistry. International Geophysics Series, 36. Academic Press, New York.

Hartle, R.E., Grebowsky, J.M., 1990. Upward ion flow in ionospheric holes on Venus. J. Geophys. Res. 95 (A1), 31–37.

Intriligator, D.S., 1989. Results of the first statistical study of Pioneer Venus plasma observations in the distant Venus tail: evidence for a hemispheric asymmetry in the pickup of ionospheric ions. Geophysical Research Letters 16 (2), 167–170.

Intriligator, D.S., Wolf, J.H., Mihalov, J.D., 1980. The Pioneer Venus orbiter plasma analyzer experiment. IEEE Trans. Geosci. Remote Sens. GE-18, 39–42.

Kallio, E., Luhmann, J.G., Lyon, J.G., 1998. Magnetic field near Venus: a comparison between Pioneer Venus Orbiter magnetic field observations and an MHD simulation. J. Geophys. Res. 103 (A3), 4753–4754.

Luhmann, J.G., Bauer, S., 1992. Solar wind effects on atmosphere evolution at Venus and Mars, 1992. In: Venus and Mars: Atmospheres, Ionospheres and Solar Wind Interactions, AGU Monograph 66, American Geophysical Union.

Luhmann, J.G., Kozyra, J.U., 1991. Dayside pickup oxygen ion precipitation at Venus and Mars: spatial distributions, energy deposition and consequences. J. Geophys. Res. 96 (A4), 5457–5467.

Mihalov, J.D., Barnes, A., 1981. Evidence for the acceleration of ionospheric O^+ in the magnetosheath of Venus. Geophys. Res. Lett. 8 (12), 1277–1280.

Mihalov, J.D., Barnes, A., 1982. The distant interplanetary wake of Venus: plasma observations from Pioneer Venus. J. Geophys. Res. 87 (A11), 9045–9053.

Moore, K.R., McComas, D.J., Russell, C.T., Mihalov, J.D., 1990. A statistical study of ions and magnetic fields in the Venus magnetotail. J. Geophys. Res. 95, 12,005–12,018.

Moore, K.R., McComas, D.J., Russell, C.T., Stahara, S.S., Spreiter, J.R., 1991. Gasdynamic modeling of the Venus magnetotail. J. Geophys. Res. 96 (A4), 5667–5681.

Nagy, A.F., Cravens, T.E., Yee, J.H., Stewart, A.I.F., 1981. Hot oxygen atoms in the upper atmosphere of Venus. Geophys. Res. Lett. 8, 629.

Russell, C.T., Snare, R.C., Means, J.D., Elphic, R.C., 1980. The Pioneer Venus Orbiter fluxgate magnetometer. IEEE Trans. Geosci. Remote Sens. GE-18, 32–36.

Vaisberg, O.L., Romanov, S.A., Smirnov, V.N., Karpinsky, I.P., Khazanov, B.I., Polenov, B.V., Bogdanov, A.V., Antonov, N.M., 1976. Ion flux parameters in the solar wind—Venus interaction region according to Venera-9 and Venera-10 data. In: Williams, D.J. (Ed.), Physics of Solar Planetary Environments. American Geophysical Union, USA.